Robust, ultrathin, and highly sensitive reduced graphene oxide/silk fibroin wearable sensors responded to temperature and humidity for physiological detection

Hyeonho Cho[a,†], Chanui Lee[a,†], ChaBum Lee[b], Sangmin Lee[a], and Sunghan Kim[a,]*

[a] School of Mechanical Engineering, Chung-Ang University, Dongjak-gu, Seoul 06974, Korea
[b] J. Mike Walker '66 Department of Mechanical Engineering, Texas A&M University, College Station, Texas 77843-3123, USA

* Corresponding Author E-mail: sunghankim@cau.ac.kr

†Hyeonho Cho and Chanui Lee contributed equally to this work.

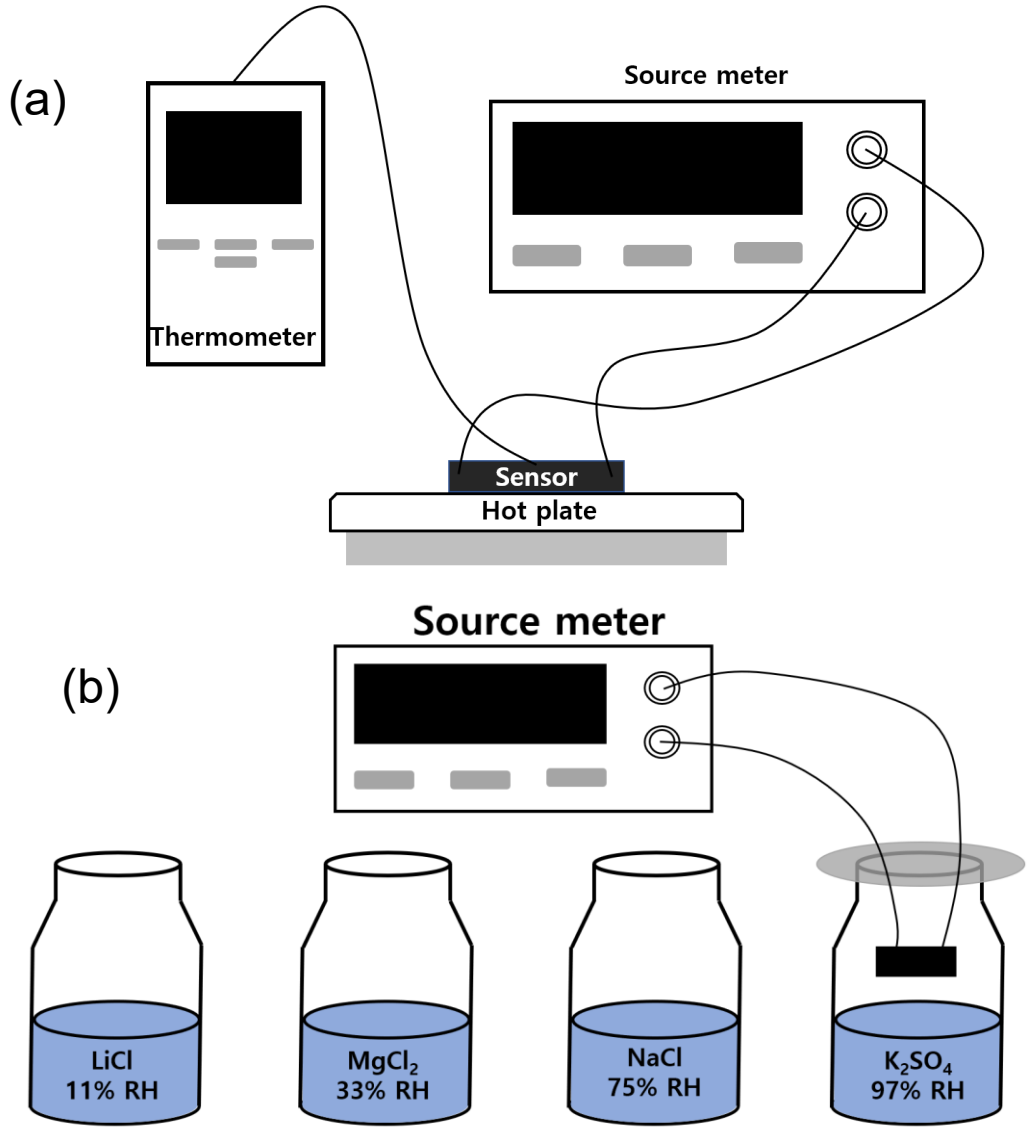

Figure S1. Schematic of the measurement methods used for the responsivity of a sensor: (a) varying the temperature and (b) varying the humidity.

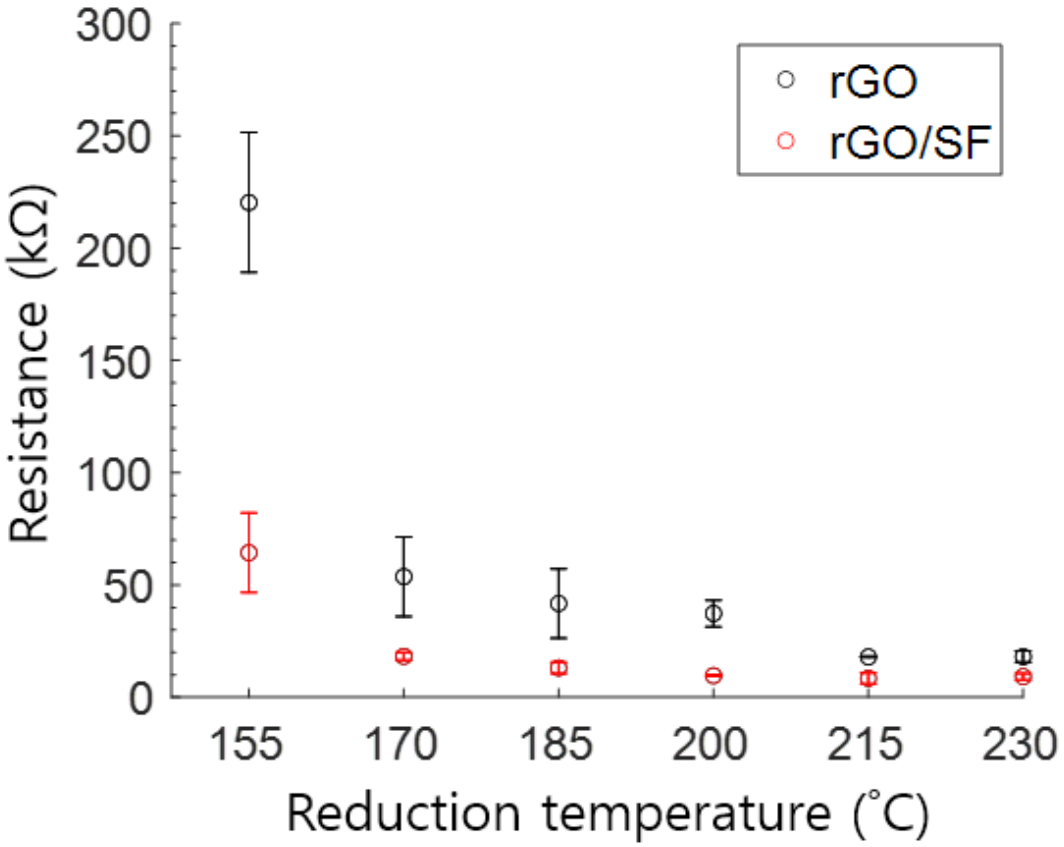

Figure S2. Resistance of rGO and rGO/SF sensors fabricated with different reduction temperatures.

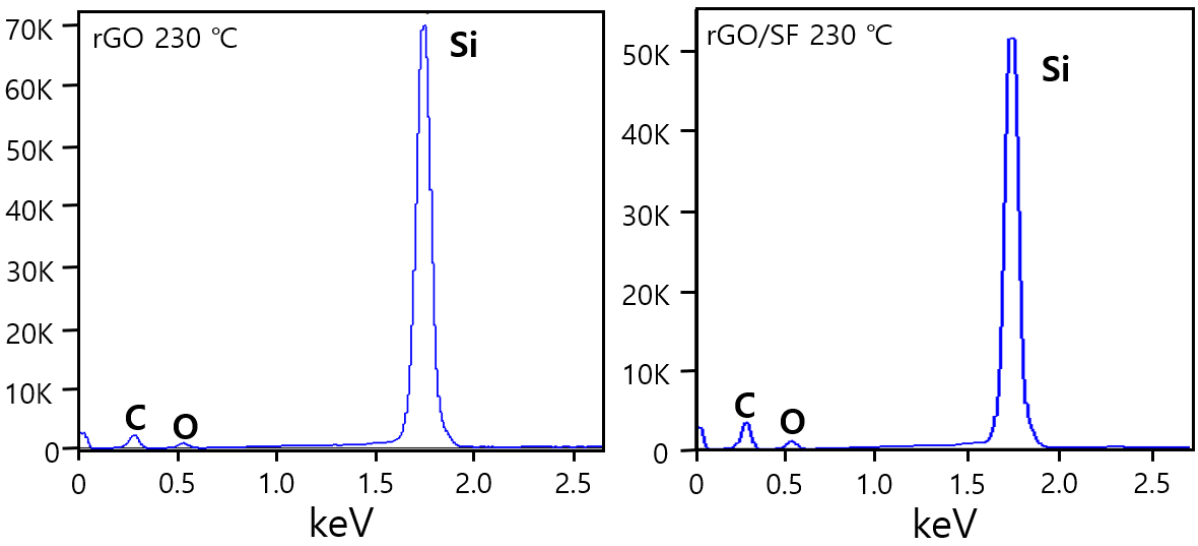

Figure S3. Representative EDS plots of rGO and rGO/SF films fabricated with a reduction temperature of 230 °C.

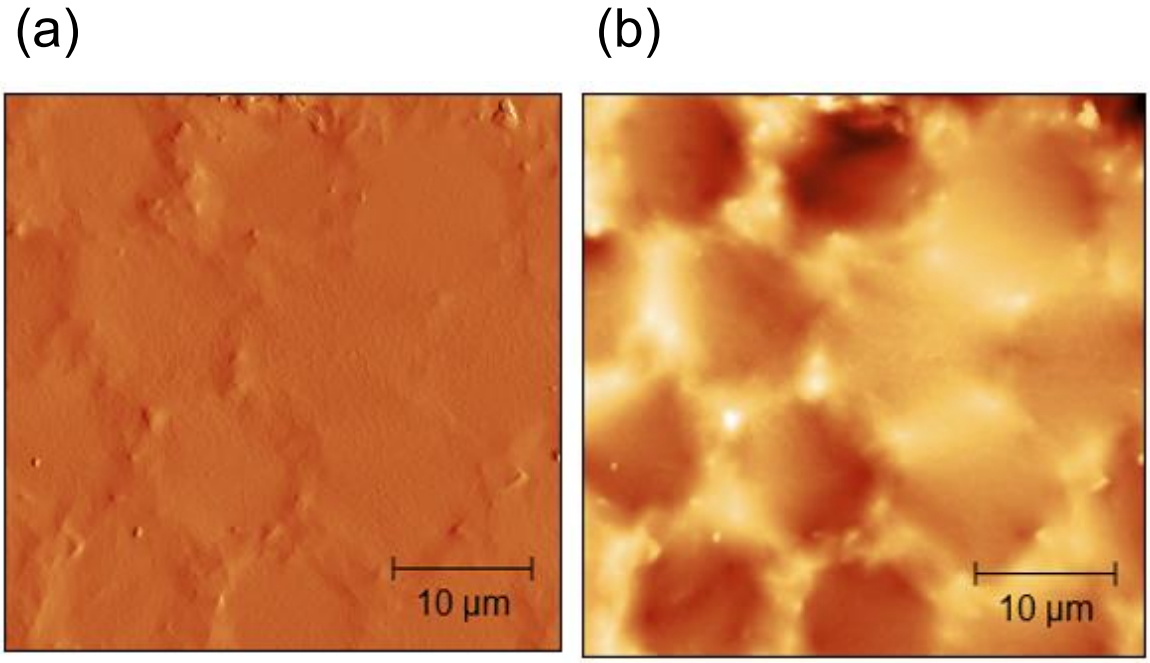

Figure S4. AFM images: (a) a force image and (b) a morphological image of an rGO/SF film scanned in the contact mode. The scale bars are 10 µm in length.

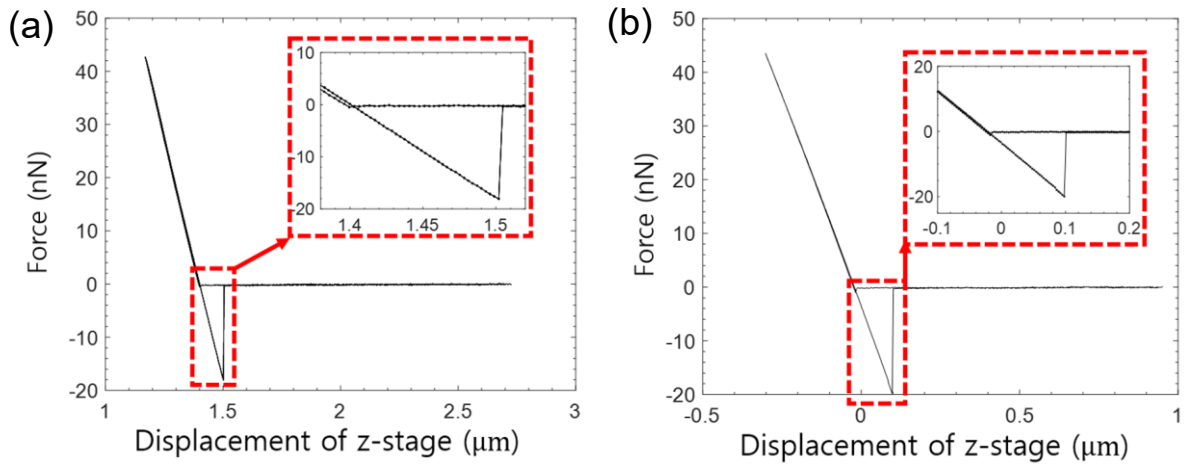

Figure S5. Force-displacement (FD) curves of the z-stage for (a) rGO and (b) rGO/SF films.

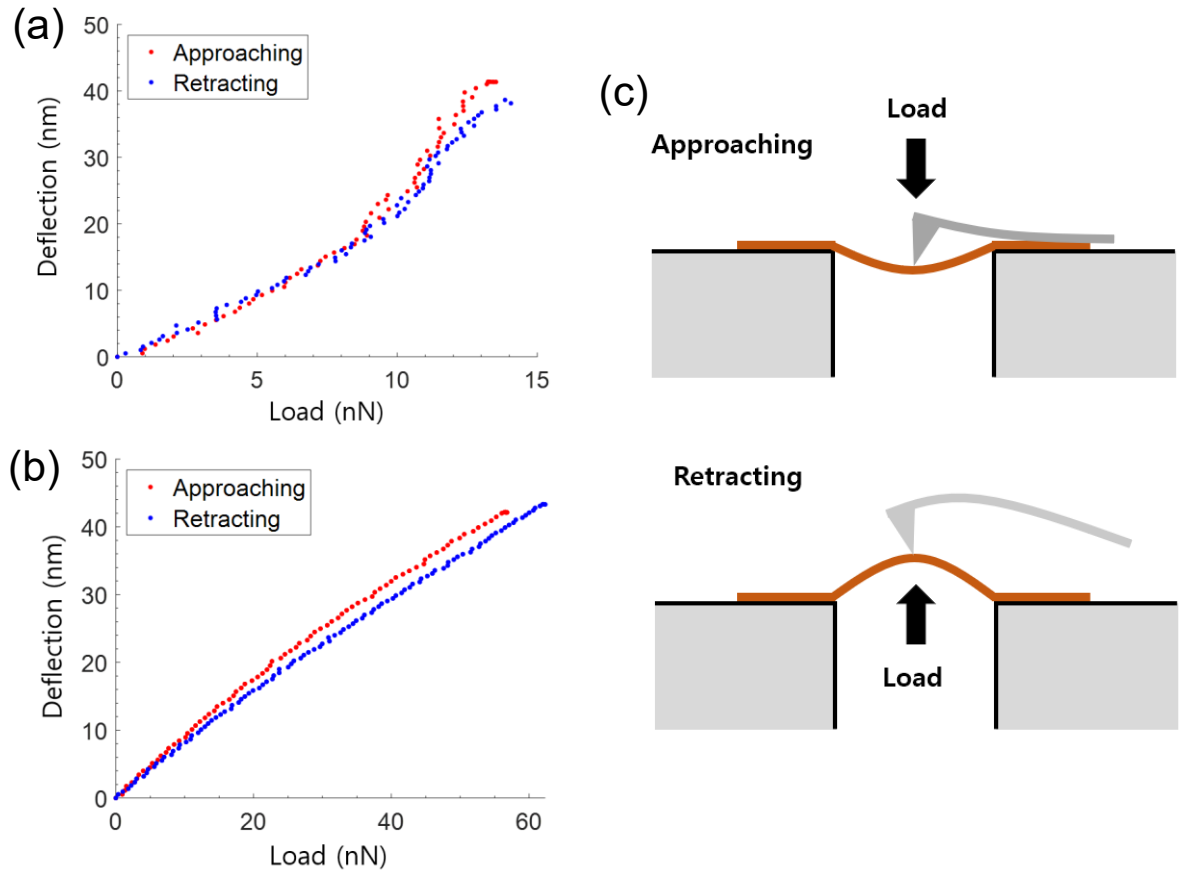

Figure S6. Load-deflection plots for (a) rGO and (b) rGO/SF films, constructed for (c) the measurement of the approaching and retracting directions.

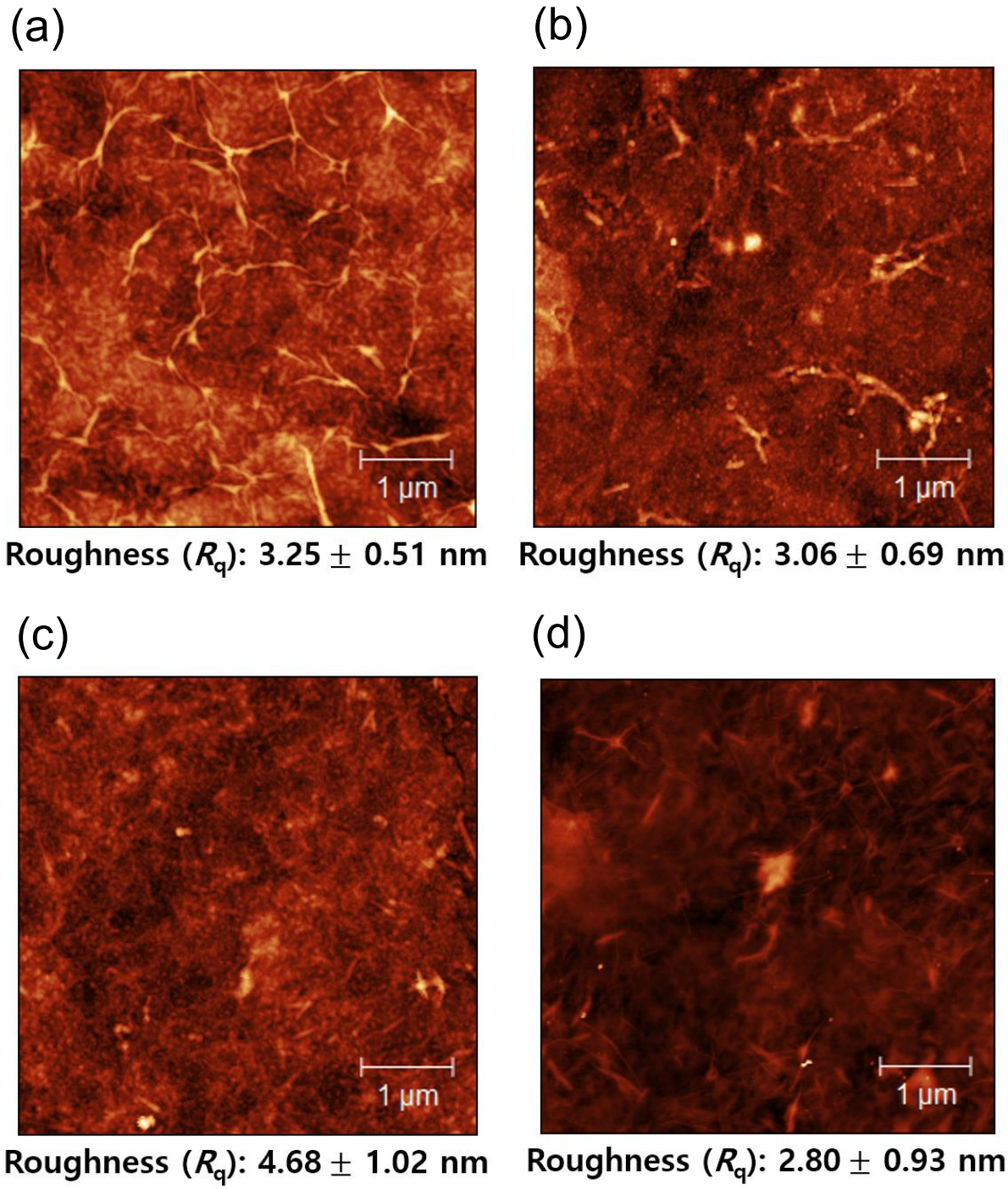

Figure S7. Morphological AFM images of rGO films fabricated with reduction temperatures of (a) 155 and (b) 230 °C. Morphological AFM images of rGO/SF films fabricated with reduction temperatures of (c) 155 and (d) 230 °C.

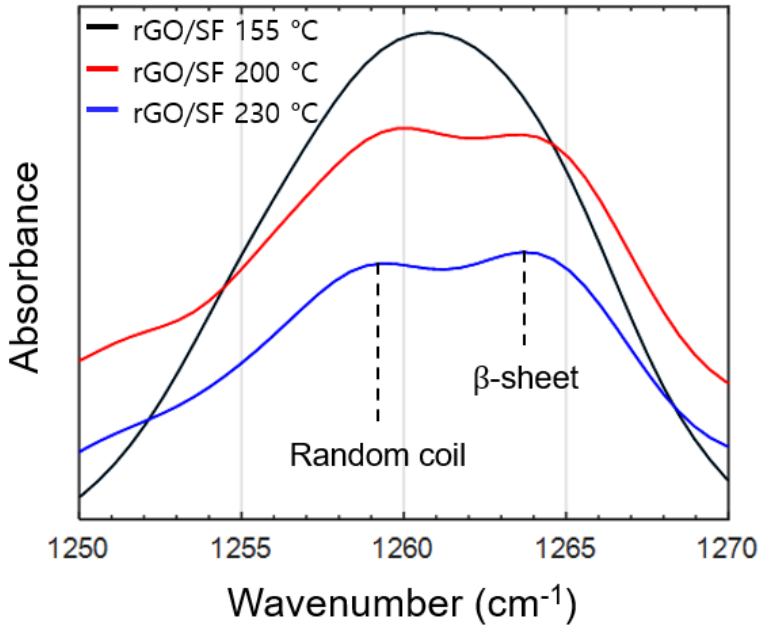

Figure S8. FTIR spectra of rGO/SF films fabricated with reduction temperatures of 155 (black), 200 (red), and 230 °C (blue).

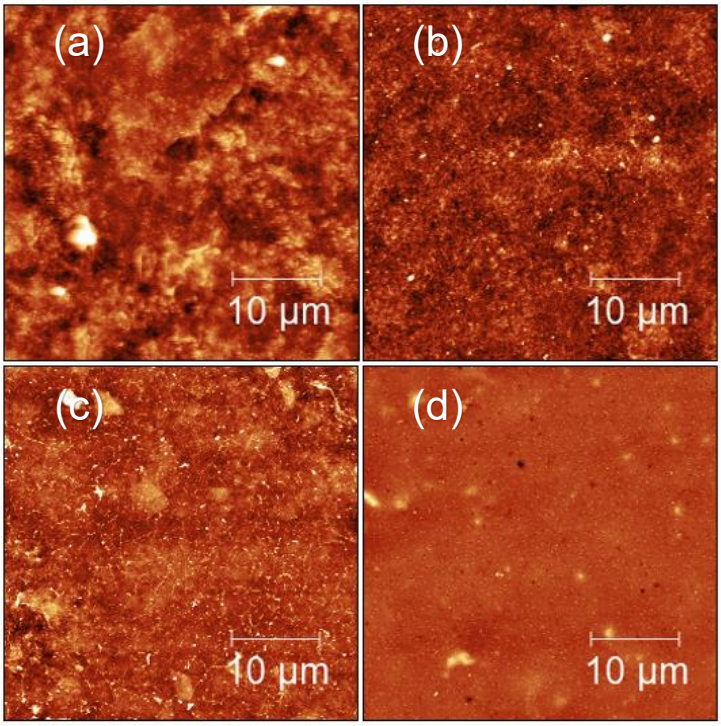

Figure S9. AFM images of (a) an rGO/SF film without an LbL structure (*z*-scale: 400 nm), (b) an rGO/SF film with an LbL structure (*z*-scale: 70 nm), (c) an rGO film (*z*-scale: 30 nm), and (d) an SF film (*z*-scale: 70 nm).

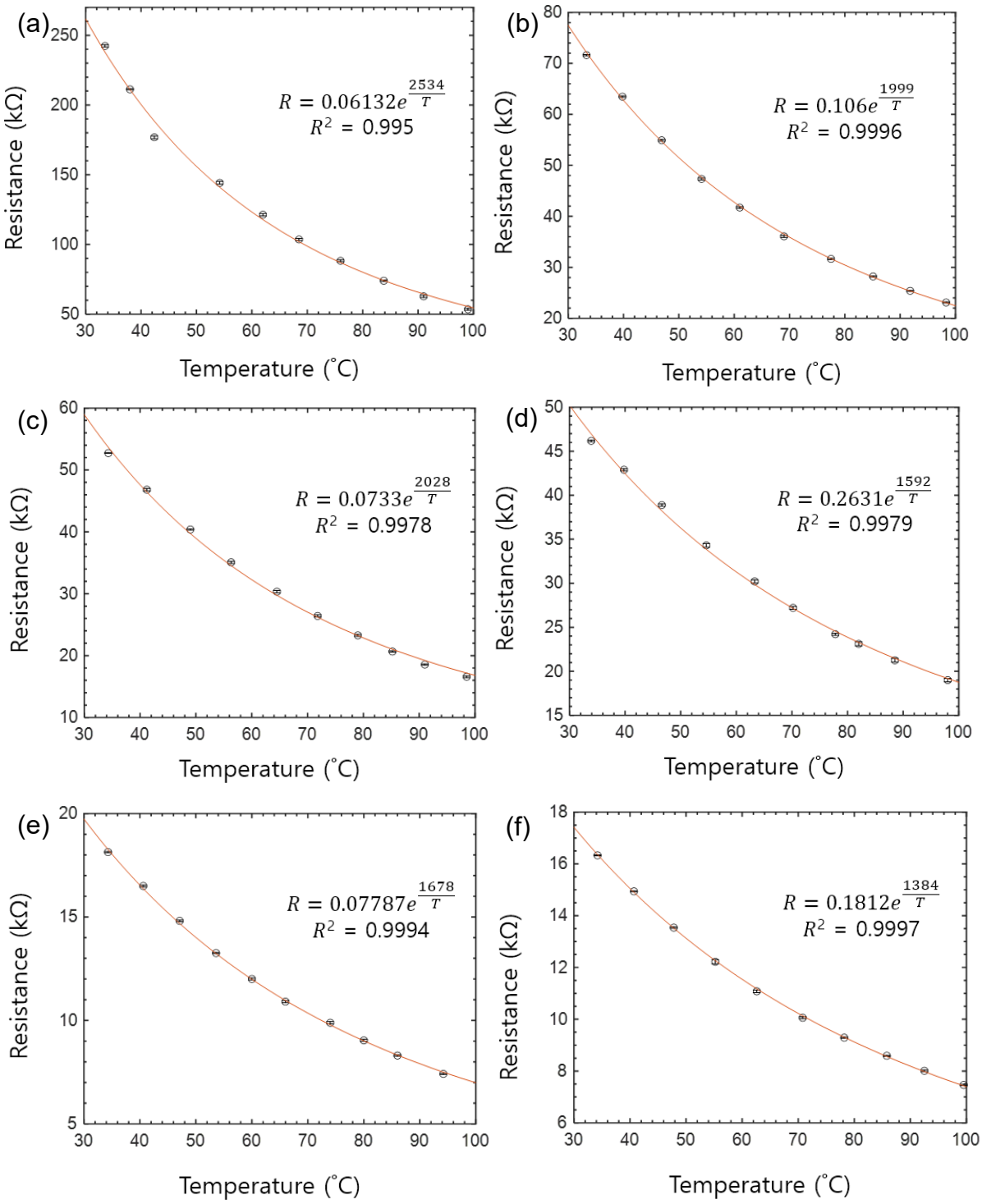

Figure S10. Resistance-temperature curves of rGO-sensor-based temperature sensors fabricated with reduction temperatures of (a) 155, (b) 170, (c) 185, (d) 200, (e) 215, and (f) 230 °C.

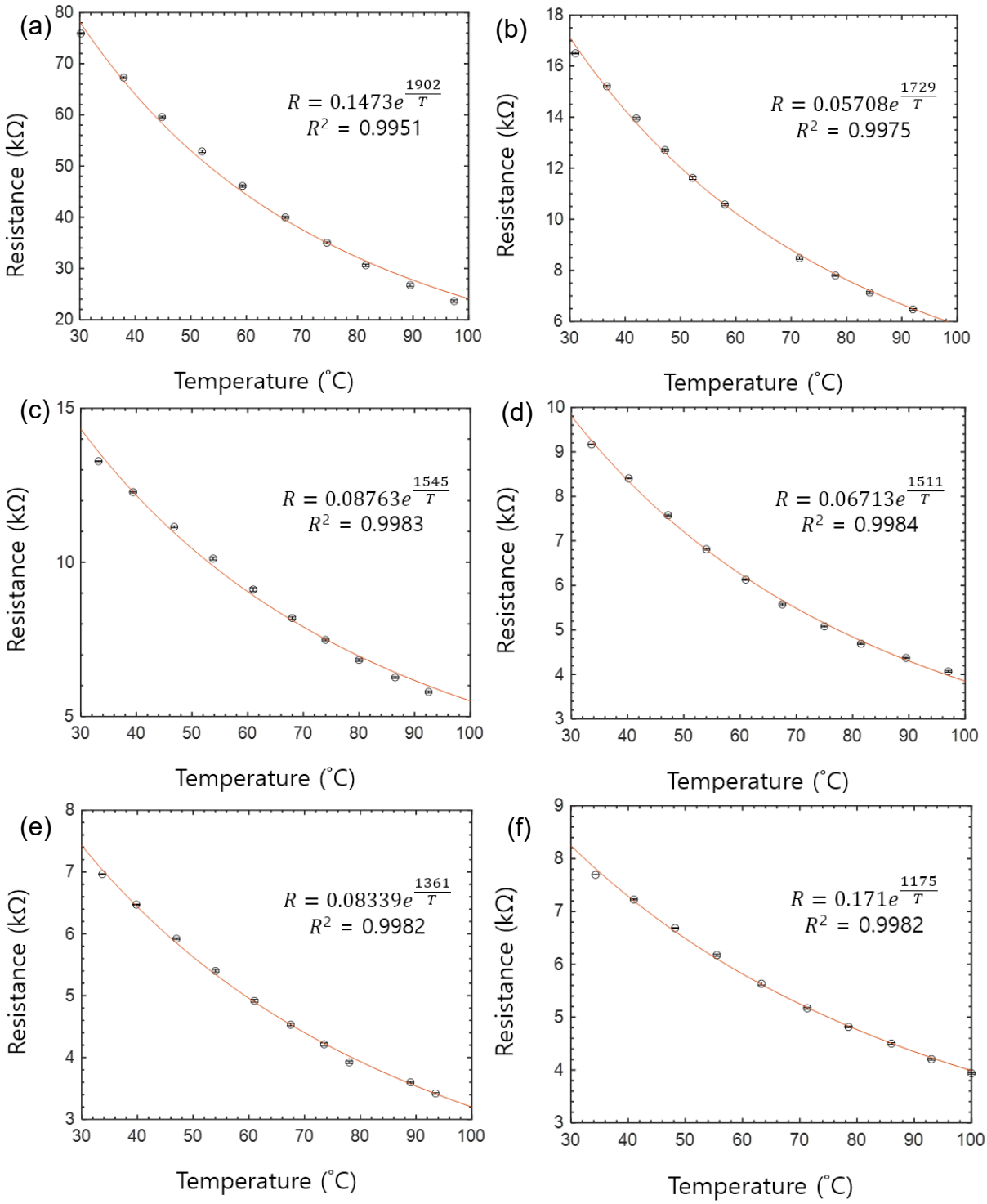

Figure S11. Resistance-temperature curves of rGO/SF-sensor-based temperature sensors fabricated with reduction temperatures of (a) 155, (b) 170, (c) 185, (d) 200, (e) 215, and (f) 230 °C.

Table S1. Specifications and comparison of some wearable temperature sensors and their performance

Sensing material	Sensitivity [%/K] at 300 K	Temp. range [˚C]	Method	Response (recovery) time(s)	Reference
rGO	0.63	30–80	Wet-spinning	7 (20)	[1]
Crosslinked PEDOT:PSS	0.77	25–50	Printing	1.5 (6)	[2]
rGO/CB	0.6	20–60	Spray-coating	100	[3]
rGO	1.30	25–45	Spray-coating	0.33	[4]
rGO/PU	1.20	30–80	Wet-spinning	7 (70)	[5]
GO/PEDOT:PSS	1.09	25–100	Printing	18 (32)	[6]
rGO-based materials	2.77	30–100	Dip-coating	5.5 (5.1)	This work

Table S2. Specifications and comparison of some wearable humidity sensors and their performance

Sensing material	Sensor type	Sensitivity	Humid. range [%RH]	Response (recovery) time(s)	Reference
rGO/CB	Resistance	161.16%	16–95	300 (100)	[3]
PDDA/RGO	Resistance	8.69%–37.43%	11–97	108–147 (94–133)	[7]
Pt-nRGO	Resistance	4.51%	6.1–66.4	-	[8]
GO	Capacitance	3215.25 pF/%RH	10–90	15.8	[9]
LIG/GO	Capacitance	9150 pF/%RH	11–97	49 (2)	[10]
rGO/ND	Capacitance	13086 pF/%RH	11–97	8 (1.5)	[11]
rGO-based materials	Resistance	48.28%	11–97	45 (40)	This work

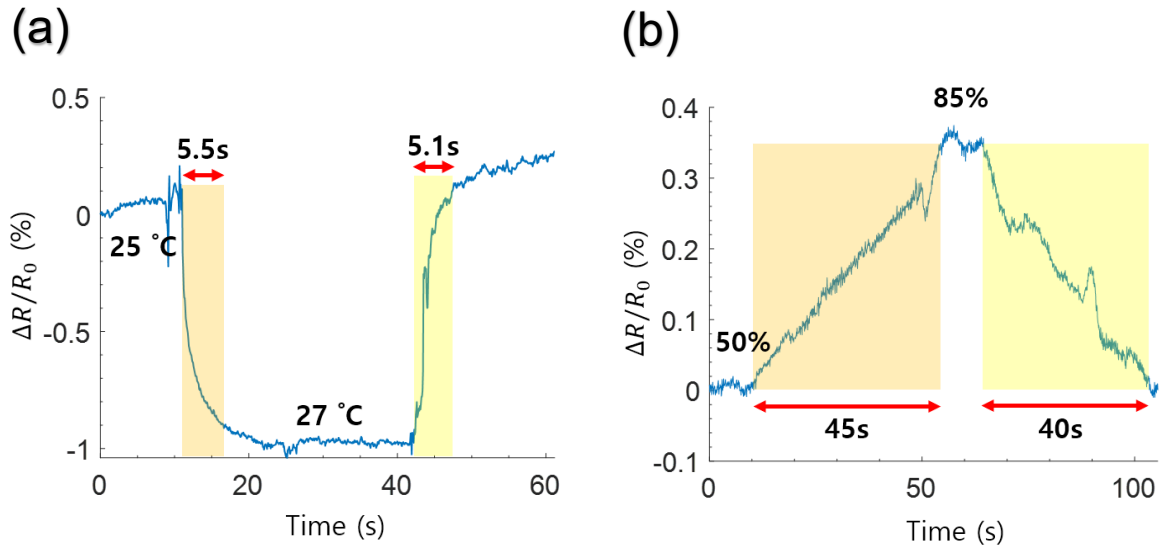

Figure S12. Response and recovery curves of the rGO/SF sensor for a reduction temperature of 170 °C: (a) between the temperatures of 25 °C to 27 °C and (b) between relative humidity values of 50% to 85%.

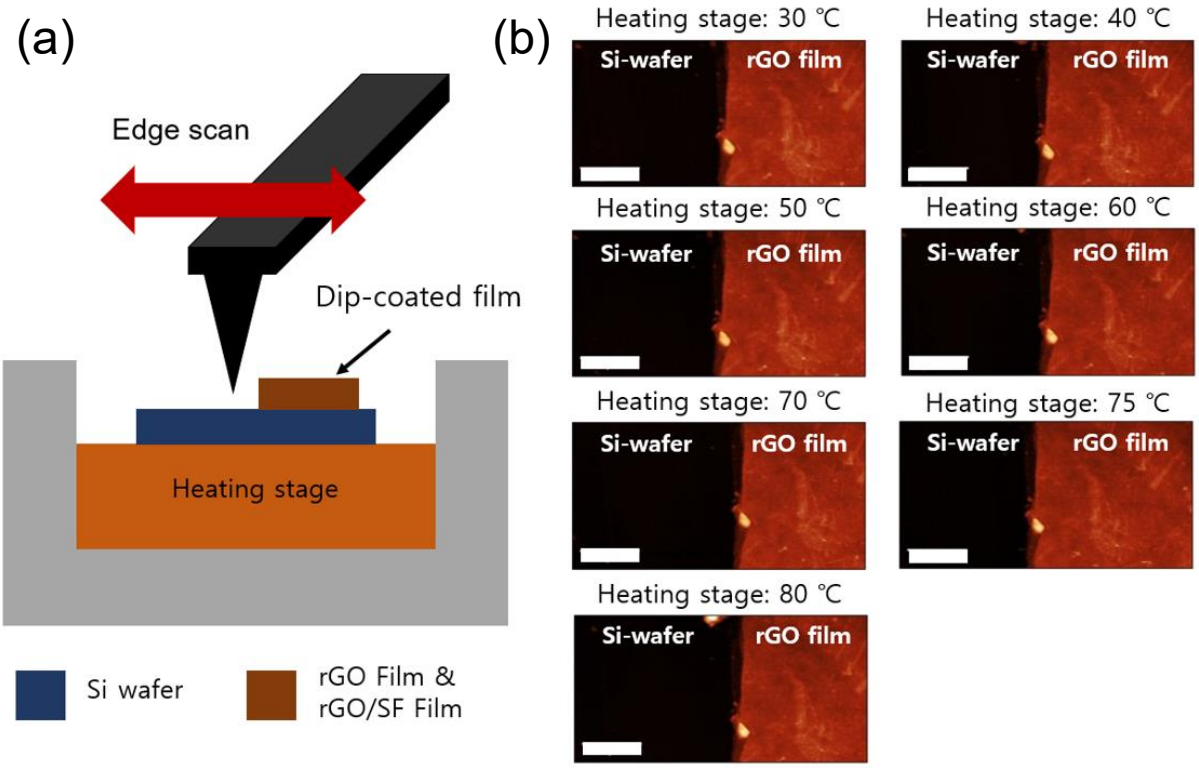

Figure S13. (a) Experimental setup used to measure the thickness of GO and rGO/SF films. (b) AFM images of the rGO film fabricated with a reduction temperature of 155 °C were obtained for various temperatures of the heating stage at a specific location. All scale bars are 2 μm.

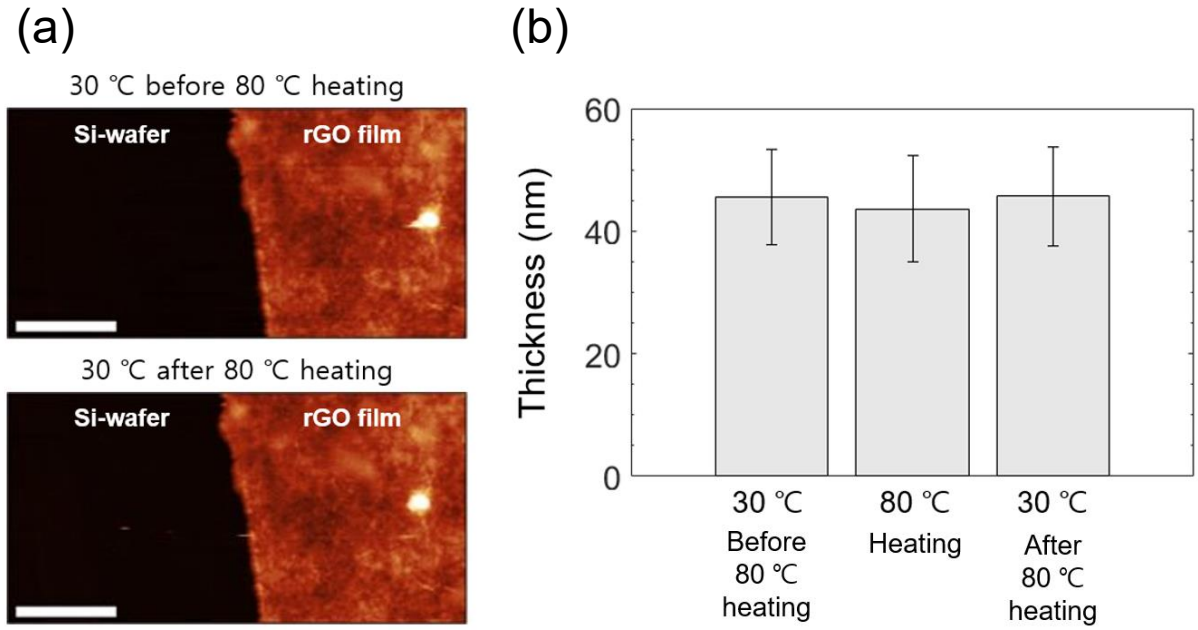

Figure S14. (a) AFM images of an rGO film at 30 °C before and after heating the film to 80 °C. (b) Thickness of the rGO film at 30 °C before heating, at 80 °C, and at 30 °C after heating and cooling. All scale bars are 3 μm.

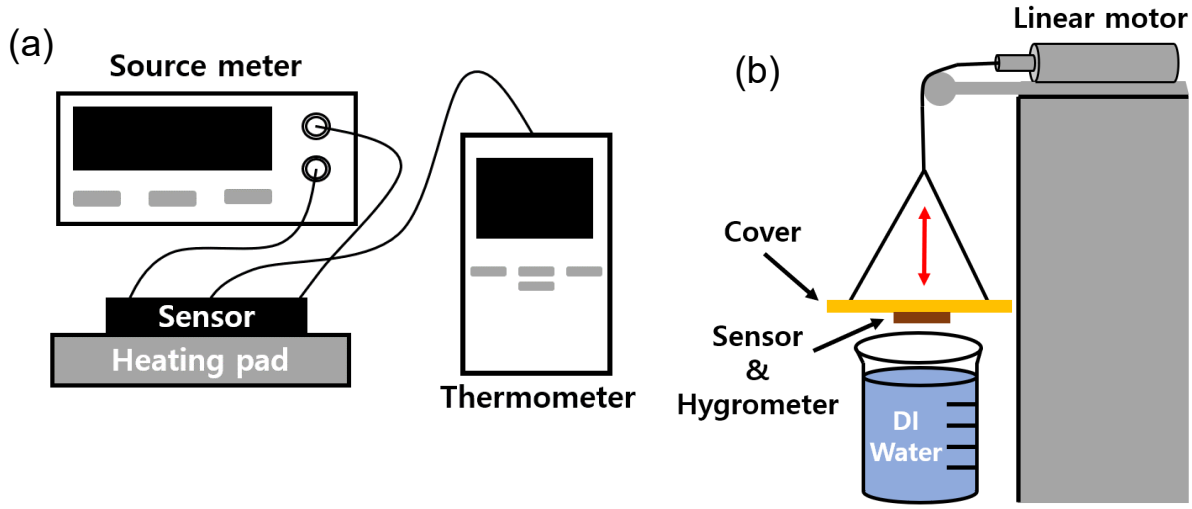

Figure S15. Schematic of the measurement methods used for the cyclic responsivity of sensors: (a) varying the temperature and (b) varying the humidity.

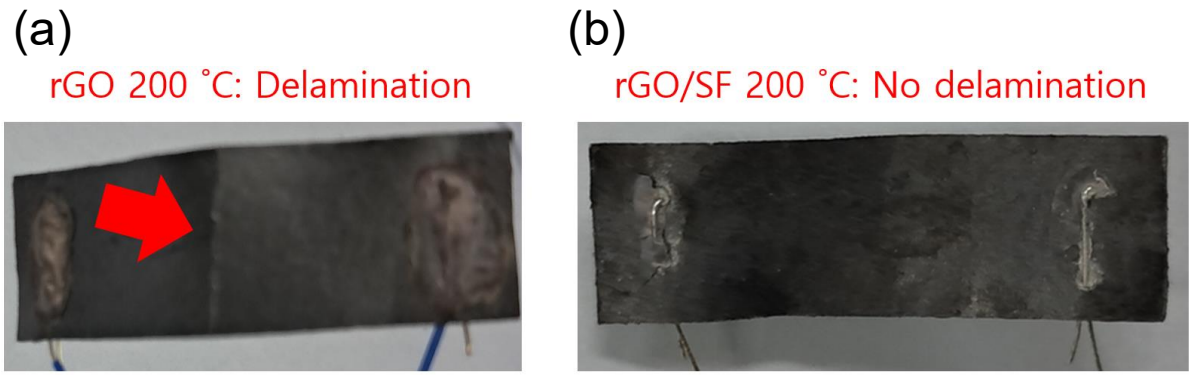

Figure S16. (a) Surface of rGO 200 °C and (b) rGO/SF 200 °C after the repeated bending test. The surface of rGO 200 °C was delaminated in the region indicated by the red arrow.

References

[1] Trung, T.-Q.; Le, H.-S.; Dang, T.-M.-L.; Ju, S.; Park, S.-Y.; Lee, N.-E. Freestanding, fiber-based, wearable temperature sensor with tunable thermal index for healthcare monitoring. *Adv. Healthc. Mater.,* **2018**, *7*, 1800074.

[2] Wang, Y.-F.; Sekine, T.; Takeda, Y.; Yokosawa, K.; Matsui, H.; Kumaki, D.; Shiba, T.; Nishikawa, T.; Tokito, S. Fully printed PEDOT: PSS-based temperature sensor with high humidity stability for wireless healthcare monitoring. *Sci. Rep.*, **2020**, *10*, 1.

[3] Liu, H.; Xiang, H.; Wang, Y.; Li, Z.; Qian, L.; Li, P.; Ma, Y.; Zhou, H.; Huang, W. A flexible multimodal sensor that detects strain, humidity, temperature, and pressure with carbon black and reduced graphene oxide hierarchical composite on paper. *ACS Appl. Mater. Interfaces*, **2019**, *11*, 40613.

[4] Liu, Q.; Tai, H.; Yuan, Z.; Zhou, Y.; Su, Y.; Jiang, Y. A high-performance flexible temperature sensor composed of polyethyleneimine/reduced graphene oxide bilayer for real-time monitoring. *Adv. Mater. Technol.*, **2019**, *4*, 1800594.

[5] Trung, T.-Q.; Dang, T.-M.-L.; Ramasundaram, S.; Toi, P.-T.; Park, S.-Y.; Lee, N.-E. A stretchable strain-insensitive temperature sensor based on free-standing elastomeric composite fibers for on-body monitoring of skin temperature. *ACS Appl. Mater. Interfaces*, **2018**, *11*, 2317.

[6] Soni, M.; Bhattacharjee, M.; Ntagios, M.; Dahiya, R. Printed temperature sensor based on PEDOT:PSS-graphene oxide composite. *IEEE Sens. J.*, **2020**, *20*, 7525.

[7] Zhang, D.; Tong, J.; Xia, B. Humidity-sensing properties of chemically reduced graphene oxide/polymer nanocomposite film sensor based on layer-by-layer nano self-assembly. *Sens. Actuator B-Chem.*, **2014**, *197*, 66.

[8] Choi, S. J.; Yu, H.; Jang, J. S.; Kim, M. H.; Kim, S. J.; Jeong, H. S.; Kim, I. D. Nitrogen-doped single graphene fiber with platinum water dissociation catalyst for wearable humidity sensor. *Small*, **2018**, *14*, 1703934.

[9] Lan, L.; Le, X.; Dong, H.; Xie, J.; Ying, Y.; Ping, J. One-step and large-scale fabrication of flexible and wearable humidity sensor based on laser-induced graphene for real-time tracking of plant transpiration at bio-interface. *Biosens. Bioelectron.*, **2020**, *165*, 112360.

[10] Zhu, C.; Tao, L. Q.; Wang, Y.; Zheng, K.; Yu, J.; Xiandong, L.; Chen, X.; Huang, Y. Graphene oxide humidity sensor with laser-induced graphene porous electrodes. *Sens. Actuator B-Chem.*, **2020**, *325*, 128790.

[11] Yu, X.; Chen, X.; Ding, X.; Chen, X.; Yu, X.; Zhao, X. High-sensitivity and low-hysteresis humidity sensor based on hydrothermally reduced graphene oxide/nanodiamond. *Sens. Actuator B-Chem.*, **2020**, *283*, 761.